Understanding Elastic Scattering

D.Das[a1],N.Deshmukh[a2],P.K.Rath[b]

[a] Saha Institute of Nuclear Physics(SINP), HBNI, 1/AF, Bidhannagar, Kolkata 700064, India

[b] Centurion University of Technology and Management(CUTM), Paralakhemundi 761211, India

Abstract

Experiments with stable-isotope beams (elastic and inelastic scattering, transfer reactions) have been successfully used to obtain information on the properties of astrophysically important states of some radioactive nuclei. We propose to study the scattering of ^{10}C with a ^{58}Ni target at $E_{Lab} = 30$ MeV ($E_{cm} = 25.0$ MeV), just around the Coulomb barrier region. The investigation of the nuclear structure of radioactive and exotic nuclei is important for nuclear astrophysics and further more elastic scattering is a very powerful tool to study the structure of exotic nuclei. The main objective here is to measure the angular distribution of the elastic cross section. With improved statistics we expect to better the previous measurements of cross section for backward angles which are very important as the surface nuclear effects are more relevant and sensitive at these angles. Also, cross-section measurements around 65° (center-of-mass framework) would be very desirable to better investigate the Fresnel diffraction peak in the angular distribution for this experimental system.

CERN-INTC-2021-023 / INTC-I-229
15/04/2021

1 Introduction and Motivation

In the present standard model we know that most of the mass in the Universe is dynamically generated by the strong interaction which can be explained by the Quantum Chromodynamics (QCD). The calculations based on statistical QCD predict that strongly interacting systems at very high energy density and/or temperature are composed of weakly interacting quarks and gluons due to asymptotic freedom and Debye screening of color charge. A thermalized system, where the properties of the system are governed by the quarks and gluons degrees of freedom is called the QuarkGluon Plasma (QGP)

[1]email : debasish.das@saha.ac.in,dev.deba@gmail.com

[2]PostDoc,SINP

and using QCD we are yet to understand the dynamics in QGP in the ongoing experiments of Relativistic Heavy Ion Collider (RHIC) and Large Hadron Collider (LHC) [1]. Another important goal the present QCD research is to understand the neutron-rich nuclear matter produced by the Radioactive Ion Beams(RIBs) since ordinary beam studies cannot adequately describe the observed phenomena of neutron stars [2] which consist of high neutron rich matter. These nuclei are produced by the RIB facility. Understanding of neutron rich matter was not enough till the RIB facilities started and from then onwards exploring the structure and the dynamics of the neutron matter is one of the prime research topics in not only nuclear physics but also astrophysics. Additionally the measurement of the reaction cross section at very low energy involving RIB beam is extremely challenging as the cross section drops rapidly below the barrier [3].

The Radioactive ion beams can provide research capabilities which are un-available with ordinary ion beams. In particular, radioactive beams allow investigation of nuclear reactions important to the stellar burning and nucleosynthesis which occur in high temperature and/or density environments in stars. The possibility of using radioactive beams for experiments in nuclear physics has made it possible to investigate the behaviour of nuclei in extreme conditions. Measurements of direct reactions with radioactive ion beams provide important information about nuclear structure as well help to elucidate nuclear structure problems and reactions of astrophysical interest. The transmission probability decreases rapidly at low energy so to understand the nature of the cross section researchers extract the astrophysical S-Factor where the important ingredient is the experimentally measured cross section. Many experimental results involving neutron rich nuclei showed that the measured cross section (or fusion cross section) are much higher compared to the predicted one, using the existing models calculations [4]. But for the proton rich nuclei there not much available data, which is another important motivation regarding this experimental proposal.

Elastic Scattering is simple and strong method which provides the rich information about the interaction potential and also the size of the interacting partners. Previous reports have shown the threshold anomaly behaviour using weakly bound nuclei [5]. As the RIB regime is close to the weakly bound nuclei one can expect the same anomalous behaviour but it has not been confirmed as there are no available experimental data. Another aim of our proposal is also to study the threshold anomalous behaviour using RIB. Besides that, the weak binding of the last bound nucleons may cause in certain special circumstances the formation of neutron (proton) skins on the surface of the nucleus and hence the formation of a halo structure. The size and the shape of the radial distribution of the nuclear matter are basic properties of nuclei and can be the most convincing evidence for the proton halo structure [6].

Elastic scattering measurements induced by light radioactive nuclei, such as ^{6}He, ^{8}B, ^{11}Be, and ^{15}C are important systems of interest in recent years, in particular at energies close to the barrier, because of the possibility of investigating surface effects and nuclear structure of the projectiles [7, 8, 9]. These radioactive nuclei have low separation energy of the valence particle and strong cluster configuration. They can produce a decoupling between the valence particle where the core can ultimately hinder the elastic scattering cross sections. Such cross-sections are very sensitive to the interaction potential between the projectile and target nuclei and to the structure of the nuclei involved. Hence the exotic structure of these light nuclei alters the elastic scattering enhancing breakup and/or transfer probabilities.

There are some reports [10] which indicates that there are many low lying resonance state which has observed for few exotic beam involving experiment in addition the coupling of many states has been incorporated to explain the final measured elastic scattering [11] data. After all the model dependent result are sensitive to parameter which some time not good to explain the result. Specially there no much data on proton rich nuclei where we want to explore. The situation looks similar to loosely bound nuclei where there are many reports which explain the importance of the breakup/transfer. But using RIB the situation may enhance due to low separations of the skin part or may be reduced due to the extended matter distribution. There is no clear picture as there are not much experimental results.

The subject of nuclear astrophysics with radioactive beams is generally sub-divided into three parts, neutron-rich nuclei [12], neutron-deficient nuclei [13] and light nuclei [14]. Since most of the applications of radioactive beams for nuclear astrophysics are in the first two categories like e.g regarding the description of the r-process in core collapse supernovae, and the hot-CNO process and rp-processes, respectively. Nuclear astrophysics with light nuclei is mainly characterized by nucleosynthesis in the Big Bang, and during the stellar hydrogen and helium burning stages. Some influence of radioactive beam techniques for hydrogen burning are detailed in the reviews [15, 16]. At certain point the hydrogen and helium fuel will be captured and converted into exotic proton rich nuclei via the rapid proton capture process [17]. So the study of proton rich nuclei is also important from the formation of element point of view .

There are some reports available for the neutron rich nuclei where the experiments has done in inverse kinematics condition to explore many aspects involving exotic nuclei [10]. There are many more data available for another group of projectile called as the weakly/loosely bound nuclei [18, 19, 20] where it has been observed that in addition with fusion there are other channel like transfer (cluster/nucleon) which plays an important role for the formation of the compound nucleus and for the fusion cross section . As the weakly bound nuclei closely resembles with the exotic beam, one can also expect the same type of behaviour. This is an important aspect of the reaction mechanism which plays a very much important role for the formation of the particles and cluster. This is another motivation to explore using the RIB beam. Since there are not much experimental data available on this study using RIB (either for neutron rich or proton rich), we want to explore this effect using the existing setup. Since RIB are exotic in nature all the predictions and observations which are true for loosely bound nuclei may fail since we have no idea what might indicate the requirement of the experimental data.

Elastic scattering using boron isotopes as projectiles has been shown to be an interesting case to investigate several effects which can be present in the process. Elastic scattering of radioactive weakly bound and proton-rich ^8B ($J^\pi = 2^+$) projectiles on a ^{58}Ni target was investigated and the coupling to the $^7Be + p$ ($S_P = 0.138$ MeV) breakup channel has shown to be crucial to describe the data [21, 22, 23]. Also, in these works, the halo configuration for ^8B could be established. Elastic scattering of stable and tightly bound ^{10}B and ^{11}B projectiles on ^{58}Ni have been recently investigated, with interesting results in terms of deformation and spin-orbit effects [24, 25].

As mentioned above the cluster structure study is an important one which can also add the emission of the alpha particle. It has been observed that in weakly bound nuclei the emission of alpha particles are more compared to what has been expected and the origin is still unknown [26]. Many reports explain that the breakup/transfer/cluster is the main origin but the full picture is still not clear. Specially while using exotic RIB beam what will be the situation is still unclear due the large extended matter distribution/halo -skin structure/low-lying resonance states. Those need to be explored. This is very important from the astrophysics point of view and also as the formation of large number of alpha particles in the star can be explained if we can able to predict what will be the situation using RIB empirically.

Although some advances have been achieved in the understanding of the nuclear interaction induced by weakly-bound and/or exotic nuclei [27, 28, 29, 30, 31, 32, 33, 34, 35], the precise description of the influence of the breakup and dynamic effects is still not completely known. In this sense, more data on elastic scattering induced by some other proton-rich nuclei such as ^{9}C, ^{10}C, ^{12}N and ^{13}O, at energies close to the barrier are required. The recent investigation of the elastic scattering of the proton-rich nucleus ^{10}C on a ^{58}Ni target at E_{Lab} = 35.3 MeV (E_{cm} = 30.0 MeV), which is close to the barrier (V_B = 27.0 MeV) [36] is hence important. The proton-rich carbon isotope ^{10}C, whose ground state has $J_{\pi} = 0^{+}$, is an interesting nucleus. It decays by three possible channels: $^{8}Be +$ ^{2}p, $^{9}B+p$, and $^{6}Be+\alpha$, with binding energies of 3.820, 4.006, and 5.101 MeV, respectively. Because the residual ^{8}Be, ^{9}B, and ^{6}Be nuclei are also un-bound by proton or α-particle decays, this nucleus can be considered to have a four-body configuration: $\alpha - \alpha - p - p$. After removing any one of these particles, the remaining nucleus also breaks apart. Due to this four-body configuration, ^{10}C is the only nucleus supposed to have a Brunnian (super-Borromean) structure [37], where the four interactions of the constituent particles can be associated with four interconnected rings. This exotic configuration has been investigated in the past at the GANIL laboratory in a breakup experiment [38] where protons and αs were detected in coincidence. For the $^{10}C +^{58} Ni$ elastic scattering experiment the measured angular distribution was analyzed with coupled-channels (CC) calculations, where projectile and target inelastic channels, as well as reorientation, were included in the coupling matrix. Also, coupled-reaction channels (CRC) and continuum-discretized coupled-channels (CDCC) calculations were performed. Since four body calculation is not available currently here we are showing a two body prediction for 9B as the exit channel only at 32 MeV as shown in Fig.1. From the Figure one can see that the 9B from the two body reaction has a complete different energy then the recoil. So the particle detector (SSB) will clearly identify the 9B and any excited state if possible. The three body and the four body observations also need to be investigated.

The proposal is to explore the above mention interesting facts about the RIB specially the following experimental investigation we want to explore using the RIB facility involving ^{10}C+^{58}Ni system.

- Elastic scattering angular distribution using ^{10}C+^{58}Ni.
- The low energy cross section measurement from which the extraction of the astrophysical S-Factor for the understanding of the reaction mechanism below the barrier.
- The breakup/transfer/cluster study involving RIB for the mentioned system. As the beam time is very precious we want to explore what ever possible from the above mentioned points. The above three items are the main aim for the mentioned reaction system. The detail for the predicted experiment has been discussed below.

Also in the same experiment [36], it was difficult to measure the different sets of energies and angular distributions in a versatile range. The cross section for the two most backward angles were very small, 15.3 and 7.5 mb/sr, and the obtained yields for the scattered ^{10}C particles were therefore small and with large error estimates. However, measurements at these backward angles are very important because the surface nuclear effects are more relevant and sensitive at these angles. Also, cross-section measurements around 65° (center-of-mass framework) would be very desirable to better investigate the Fresnel diffraction peak in the angular distribution for this experimental system.

2 Experimental Proposal

Since in the experimental data of ^{10}C+^{58}Ni reaction there was data for the elastic scattering angular distribution in some angles [36]. So we are proposing a complete set of measurement to understand the full dynamics. Further measurements which we want to perform also are as follows:

- elastic scattering angular distribution of ^{10}C+^{58}Ni in 5 set of energy. As the average barrier is 27.5 MeV we want to investigate at 24, 26, 28, 30, 32 MeV energies such that both above and below the barrier energy range can be explored.
- The detection of the evaporated/breakup/charge particles in coincidence to understand the transfer/breakup mechanism.
- The measurement of cross fusion section.

The detail of each proposals are also explained below. At the five energies (24,26,28,30,32 MeV) which we want to investigate since the average barrier is 27.5MeV. In each energy we want to cover forward and back ward angle. If not all possible but we need 50,120,130,140 angles such that we can compare the data-sets with the ones measured with smaller uncertainties. Calculations of Rutherford cross-section for the above energy and angles are shown in Table.1.

We propose to study the scattering of ^{10}C with a ^{58}Ni target at E_{Lab} = 30 MeV (E_{cm} = 25.0 MeV), just around the Coulomb barrier region for this experimental set-up. The main objective is to measure the angular distribution of the elastic cross section. As obtained earlier [36], we expect strong couplings between the elastic, transfer and direct breakup channels. The elastic data will be analyzed, in a first approach, by means of the optical model and polarization potentials to extract the relevant information. The explicit effects due to transfer and breakup mechanism can be studied by the Coupled Channel calculations (CRC, CDCC). If properly tuned, the breakup process can be included in the optical potentials describing the entrance and exit channels in the CRC calculation, and the transfer process in the CDCC calculation, allowing for both calculations to reproduce in a consistent manner the measured angular distribution of the elastic scattering.

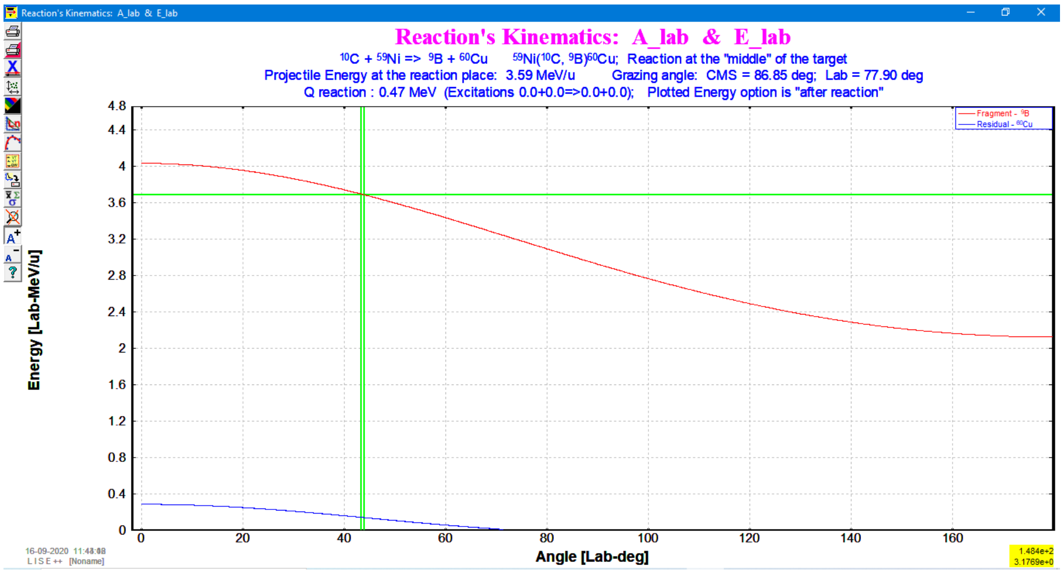

Figure 1: Two body reaction with 9B as output

Also the aim can be set to extract the total reaction cross section in addition to the measurement of the elastic scattering, so as to obtain information on the relative contribution of transfer and break-up cross-sections [33, 34, 35]. As cross sections are influenced by the atomic and mass numbers of the colliding nuclei, to compare data of different systems it is necessary to apply some reduction procedure. The reduction is made from the collision energy and cross sections point of view to weaken, or completely eliminate (if possible), the atomic and mass numbers effect. Recently [39], a new reduction procedure (N) has been proposed and successfully applied to many different projectile and medium mass systems [40, 41]that allows to access to the quantitative effect of the direct reaction mechanism on the total reaction cross section by comparing the reduced cross section of tightly and weakly bound systems.

3 Yield Estimation

The measurement of fusion cross section is another important quantity to understand the reaction mechanism. It will also help to understand the behaviour of the cross-section below the barrier, where the transmission goes down drastically. In addition since it is exotic in nature, the coupling effect can play significant role and try to enhance the fusion.

But unless we measure and have the experimental data it will not be easy to understand. So in this proposal we also want to measure the fusion cross section from the α channel . The same α can come from the evaporation of the equilibrated compound nucleus or may be from the transfer or breakup, but the energy spectra will be different. Hence, based on the energy identification the origin can be identified and the total cross section will be extracted. The predicted fusion cross section for the current system has been shown in Table. 3. The calculations are done using PACE4 (a Statistical model analysis of Compound Nucleus decay). From the Table one can see that the cross section is not very low and hence measurable.

In Fig.2 and Fig.3, we show the results of an estimate for the angular distribution calculated with FRESCO code and using the bare Sao Paulo Potential. Considering the parameters in the table below we can get for all the angles a yield(Y) rate of Y/hour=0.0374$\times$(dσ/dΩ). Yields after 24 hours run are given in the Table.2 (at the end). For all the five sets of energy we need accordingly more time. The calculation here we have shown for the two beam energies for which the last energy is shown at 33 MeV, in-order to have a rough estimate of the higher-side of the counts which we might need to accomplish our research.

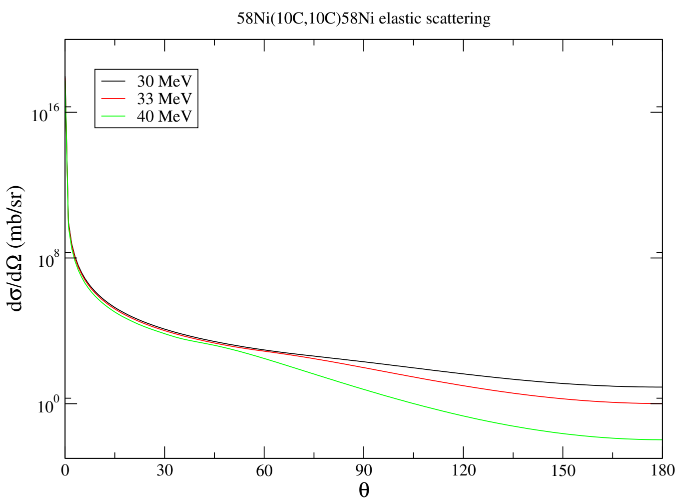

Figure 2: Elastic scattering cross-section vs. lab-angle.

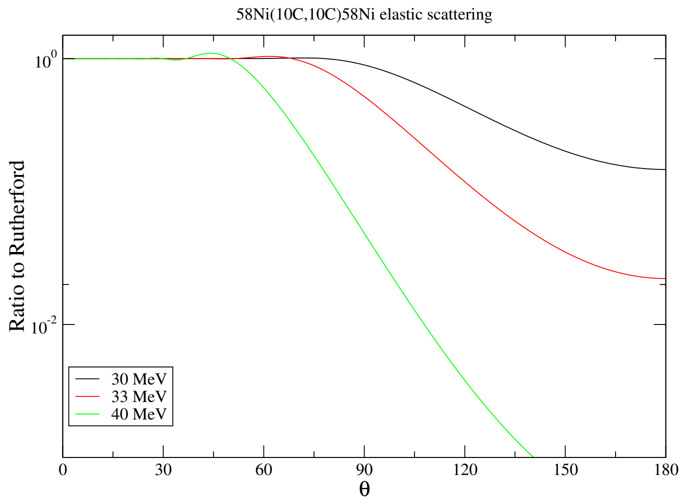

Figure 3: Ratio to Rutherford cross-section vs. lab-angle.

4 Detectors

A small calculation has been done to understand the detector configuration. Since the aim is to measure the full angular distribution which clearly identify the elastic peak, a ΔE-E configuration is needed. The lowest energy is 24 MeV for incident beam and the scattered particle in forward is ∼20 MeV at 20 ° and in the back angle of ∼120 ° is at 12 MeV. In the above energy range of the scattered particle, it will be detected if the ΔE thickness is ∼5 micron or less and the E part can be of 300 micron to stop the particle completely. As the plan is to measure the particle spectra and also for this purpose the same E-ΔE configuration will work. Assuming the two body break up and further considering α be one breakup fragments, the maximum energy will be 10 MeV using the mass energy relation, which can be detected by same ΔE configuration having thickness 5 micron or less. Hence telescopes will be required to reduce the beam time and also to cover larger angular setting at a time. But based on the availability of the detectors the time of the experiment the configuration can be modified keeping the above criteria fixed.

5 Summary

In summary we are proposing to investigate the $^{58}Ni(^{10}C,^{10}C)^{58}Ni$ elastic scattering at 30 and 33 MeV (lab frame) using a total 10 days of machine time. The scattered ^{10}C particles are to be detected by Silicon Surface barrier detectors in a telescopic arrangement (ΔE-E) at forward angles (20,30,45,60,70 °) and at backward angles (80,90,100,110,120 °) for both the set of energies. Here the angles may vary as per the grazing angles of the respective energies. For instance the grazing angle for E_{lab} = 30 MeV is $\theta_{lab(gr)}$ = 132 ° and for E_{lab} = 33 MeV is $\theta_{lab(gr)}$ = 93 °. Thus, if we accomplish 5 days of dedicated run respectively for each energy set, we will roughly expect to obtain the statistical errors ranging from 0.5% to 10% starting from the most forward to the most backward angles. Such errors were quite high in the previous experimental attempt [36].

References

[1] D. Das and N. Dutta, Int. J. Mod. Phys. A **33**, no. 16, 1850092 (2018)

[2] D. Das [STAR Collaboration], arXiv:0906.0630 [nucl-ex].)

[3] B. B. Back, J. A. Clark, R. C. Pardo, K. E. Rehm and G. Savard, AIP ADVANCES 4, 041005 (2014).

[4] Raj Kumar, Deepika Jain, Nuclear Physics A 929 (2014) 169183.

[5] I. Martel *et.al.*, Nuclear Physics A 582 (1995) 357-368.

[6] A.V. Dobrovolsky *et.al.*, Nuclear Physics A 989 (2019) 4058.

[7] L.F. Canto, P.R.S. Gomes, R. Donangelo, J. Lubian and M.S. Hussein, Phys. Rep. 596, 1 (2015).

[8] J. J. Kolata, V. Guimares and E. F. Aguilera, Eur. Phys. J. A 52, 123 (2016).

[9] N. Keeley, K.W. Kemper and K. Rusek, Phy. Rev. C 88, 017602 (2013).

[10] A. Sanetullaev, R. Kanungo *et.al.*, Physics Letters B 755 (2016) 481485.

[11] V. Guimares, *et.al.*, PHYSICAL REVIEW C 100, 034603 (2019).

[12] K. Hebeler, J. D. Holt, J. Menendez and A. Schwenk, Ann. Rev. Nucl. Part. Sci. **65**, 457 (2015)

[13] K. Langanke and H. Schatz, Phys. Scr. T152 014011 (2013).

[14] H.O.U Fynbo, Phys. Scr. 2013 014010 (2013).

[15] E. G. Adelberger et al. Rev. Mod. Phys. 83, 195 (2011).

[16] J. Jose and C. Illiadis, Rep. Prog. Phys. 74 096901 (2011).

[17] H. Schatz and K.E. Rehm, Nuclear Physics A 777 (2006) 601622.

[18] D. H. Luong *et.al.*, EPJ Web of Conferences , 000 (2011).

[19] D. H. Luong *et.al.*, EPJ Web of Conferences 35, 05007 (2012).

[20] P. K. Rath *et.al.*, PHYSICAL REVIEW C 88, 044617 (2013).

[21] E.F. Aguilera *et.al.*, Phys. Rev. C 79, 021601 (R) (2009).

[22] E.F. Aguilera, I. Martel, A.M. Snchez-Bentez, and L. Acosta, Phys. Rev. C 83, 021601 (R) (2011).

[23] J. Lubian et al., Phys. Rev. C 79, 064605 (2009).

[24] V. Scarduelli et al., Phys. Rev. C 96, 054610 (2017).

[25] N.N. Deshmukh et al., Phys. Rev. C 92, 054615 (2015).

[26] P. K. Rath *et.al.*, EPJ Web of Conferences 86, 00037 (2015).

[27] N. Keeley, R. Raabe, N. Alamanos, and J.L. Sida, Prog. Part Nucl. Phys. 59, 579 (2007).

[28] N. Keeley, N. Alamanos, K.W. Kemper, and K. Rusek, Prog. Part Nucl. Phys. 63, 396 (2009).

[29] K. Hagino and N. Takigawa, Prog. Theor. Phys. 128, 1061 (2012).

[30] V. Guimares et al., Phys. Rev. C 75, 054602 (2007).

[31] R. Kanungo et al., Phys. Lett. B 660, 26 (2008).

[32] H.B. Jeppesen et al., Phys. Lett. B 642, 449 (2006).

[33] N.N. Deshmukh et al., Phys. Rev. C 83, 024607 (2011).

[34] N.N. Deshmukh et al., Eur. Phys. J. A 47, 118 (2011).

[35] S. Mukherjee et al., Eur. Phys. J. A 45, 23 (2010).

[36] V. Guimares et al., Phys. Rev. C 100, 034603 (2019).

[37] https://knotplot.com/brunnian/

[38] N. Curtis et al., Phys. Rev. C 77, 021301(R) (2008).

[39] V. Morcelle et al., Phys. Rev. C 95, 014615 (2017).

[40] N. Deshmukh and J. Lubian, Eur. Phys. J A 54, 101 (2018).

[41] N. Deshmukh, J. Lubian and S. Mukherjee, Eur. Phys. Lett. 127, 12001 (2019).

Table 1: The predicted elastic cross-section at the proposed energy.

Energy of Projectile	Scattering Angle(Rutherford scattering differential cross-section)
24 MeV	50 °(($d\sigma/d\Omega$) $\sim$ 1990 mb/sr)
24 MeV	120 °(($d\sigma/d\Omega$) $\sim$ 109 mb/sr)
24 MeV	130 °(($d\sigma/d\Omega$) $\sim$ 90.3 mb/sr)
24 MeV	140 °(($d\sigma/d\Omega$) $\sim$ 77.7 mb/sr)
26 MeV	50 °(($d\sigma/d\Omega$) $\sim$ 1690 mb/sr)
26 MeV	120 °(($d\sigma/d\Omega$) $\sim$ 93 mb/sr)
26 MeV	130 °(($d\sigma/d\Omega$) $\sim$ 77 mb/sr)
26 MeV	140 °(($d\sigma/d\Omega$) $\sim$ 66.2 mb/sr)
27.47 MeV	50 °(($d\sigma/d\Omega$) $\sim$ 1520 mb/sr)
27.47 MeV	120 °(($d\sigma/d\Omega$) $\sim$ 83.3 mb/sr)
27.47 MeV	130 °(($d\sigma/d\Omega$) $\sim$ 69 mb/sr)
27.47 MeV	140 °(($d\sigma/d\Omega$) $\sim$ 59.3 mb/sr)
28 MeV	50 °(($d\sigma/d\Omega$) $\sim$ 1460 mb/sr)
28 MeV	120 °(($d\sigma/d\Omega$) $\sim$ 80.2 mb/sr)
28 MeV	130 °(($d\sigma/d\Omega$) $\sim$ 66.4 mb/sr)
28 MeV	140 °(($d\sigma/d\Omega$) $\sim$ 57.1 mb/sr)
30 MeV	50 °(($d\sigma/d\Omega$) $\sim$ 1270 mb/sr)
30 MeV	120 °(($d\sigma/d\Omega$) $\sim$ 69.8 mb/sr)
30 MeV	130 °(($d\sigma/d\Omega$) $\sim$ 57.8 mb/sr)
30 MeV	140 °(($d\sigma/d\Omega$) $\sim$ 49.7 mb/sr)
32 MeV	50 °(($d\sigma/d\Omega$) $\sim$ 1120 mb/sr)
32 MeV	120 °(($d\sigma/d\Omega$) $\sim$ 61.4 mb/sr)
32 MeV	130 °(($d\sigma/d\Omega$) $\sim$ 50.8 mb/sr)
32 MeV	140 °(($d\sigma/d\Omega$) $\sim$ 43.7 mb/sr)

Table 2: Counts estimation for 24 hours run, angles in lab frame.

solid angle	$\sim$ 10 msr
^{58}Ni Target thickness	$\sim 2\ mg/cm^2$
^{10}C beam intensity	5×10^4 pps
Energy	30 MeV
Jacobian	0.8 forward angles, 1.0 backward angles
20 °((dσ/dΩ) $\sim$ 60000 mb/sr)	$\sim$ 53000 counts
30 °((dσ/dΩ) $\sim$ 12000 mb/sr)	$\sim$ 10000 counts
45 ° ((dσ/dΩ) $\sim$ 2500 mb/sr)	$\sim$ 2200 counts
60 °((dσ/dΩ) $\sim$ 900 mb/sr)	$\sim$ 800 counts
70 °((dσ/dΩ) $\sim$ 500 mb/sr)	$\sim$ 400 counts
80 °((dσ/dΩ) $\sim$ 300 mb/sr)	$\sim$ 250 counts
90 °((dσ/dΩ) $\sim$ 200 mb/sr)	$\sim$ 150 counts
100 °((dσ/dΩ) $\sim$ 100 mb/sr)	$\sim$ 90 counts
110 °((dσ/dΩ) $\sim$ 70 mb/sr)	$\sim$ 60 counts
120 °((dσ/dΩ) $\sim$ 40 mb/sr)	$\sim$ 35 counts
Energy	33 MeV
20 °((dσ/dΩ) $\sim$ 50000 mb/sr)	$\sim$ 44000 counts
30 °((dσ/dΩ) $\sim$ 10300 mb/sr)	$\sim$ 9200 counts
45 ° ((dσ/dΩ) $\sim$ 2000 mb/sr)	$\sim$ 1700 counts
60 °((dσ/dΩ) $\sim$ 750 mb/sr)	$\sim$ 650 counts
70 °((dσ/dΩ) $\sim$ 400 mb/sr)	$\sim$ 350 counts
75 °((dσ/dΩ) $\sim$ 290 mb/sr)	$\sim$ 260 counts
80 °((dσ/dΩ) $\sim$ 200 mb/sr)	$\sim$ 180 counts
85 °((dσ/dΩ) $\sim$ 140 mb/sr)	$\sim$ 125 counts
90 °((dσ/dΩ) $\sim$ 90 mb/sr)	$\sim$ 80 counts
95 °((dσ/dΩ) $\sim$ 60 mb/sr)	$\sim$ 55 counts
100 °((dσ/dΩ) $\sim$ 40 mb/sr)	$\sim$ 35 counts

Table 3: Total and Residual nuclei cross-section at the proposed energy.

Energy of Projectile(MeV)	Total cross-section(mb)	Residual nuclei cross-section(mb)
24.00	0.0059	0.0000874
26.00	0.194	0.000833
27.47	2.48	0.00892
28.00	6.04	0.00966
30.00	79.2	0.554
32.00	219	0.241